PHYSICAL REVIEW B **85**, 161201(R) (2012)

Fully ordered Sr_2CrReO_6 epitaxial films: A high-temperature ferrimagnetic semiconductor

A. J. Hauser,[1] J. R. Soliz,[2] M. Dixit,[3] R. E. A. Williams,[3] M. A. Susner,[3] B. Peters,[1] L. M. Mier,[2] T. L. Gustafson,[2] M. D. Sumption,[3] H. L. Fraser,[3] P. M. Woodward,[2] and F. Y. Yang[1,*]

[1]*Department of Physics, The Ohio State University, Columbus, Ohio 43210-1117, USA*

[2]*Department of Chemistry, The Ohio State University, Columbus, Ohio 43210-1117, USA*

[3]*Department of Materials Science and Engineering, The Ohio State University, Columbus, Ohio 43210-1117, USA*

(Received 21 November 2011; revised manuscript received 21 March 2012; published 3 April 2012)

We report growth of Sr_2CrReO_6 epitaxial films with 99% Cr/Re ordering and crystalline perfection comparable to those of high-quality semiconductor films. The Sr_2CrReO_6 films show a Curie temperature of 508 K and a saturation magnetization of 1.29 μ_B per formula unit, which confirms the presence of strong spin-orbit coupling. Unexpectedly, electrical transport and optical absorption measurements indicate that Sr_2CrReO_6 is a semiconductor with a band gap of 0.21 eV. The unique combination of high temperature ferrimagnetism and semiconductivity is both scientifically interesting and highly attractive for applications.

DOI: 10.1103/PhysRevB.85.161201 PACS number(s): 75.50.Pp, 68.37.Ma, 75.50.Gg, 75.70.Tj

Utilization of the spin degree of freedom in metals and semiconductors has the potential to create myriad new advances over current charge-based technologies.[1–3] Half-metallic spin injectors and magnetic semiconductors will be essential components for realizing these next generation technologies.[3–6] The main barrier to this technological breakthrough has been finding materials that exhibit ferromagnetic ordering and spin polarized transport above room temperature.

The $A_2BB'O_6$ double perovskites (DP) have been extensively studied due to their high spin polarization (P) and Curie temperatures (T_C) well above room temperature, both characteristics needed for practical spintronic applications.[7,8] However, the fabrication of high-quality DP epitaxial films has proven challenging, especially for attaining high levels of B/B' ordering, which is essential for their desirable properties. This problem has been a major roadblock in the development of DP epitaxial films for use in spintronics.[9] Sr_2CrReO_6 (SCRO) is considered a promising material for spintronics due to its high T_C of 635 K and predicted half-metallicity with an expected saturation magnetization (M_S) of 1 μ_B per formula unit (f.u.).[10–18] All calculations predict metallic conductivity, but when spin-orbit coupling is included Sr_2CrReO_6 becomes a pseudo-half-metal with spin polarization $P \sim 90\%$ and the M_S increases to 1.28 μ_B/f.u.[19] To date, the highest M_S reported for Sr_2CrReO_6, in either bulk or film samples, is 1.01 μ_B/f.u.,[17] which can either be taken as evidence for negligible spin-orbit coupling or attributed to the effects of Cr/Re antisite disorder.

Stoichiometric phase-pure Sr_2CrReO_6 powders were made via the conventional solid-state chemical synthesis using evacuated sealed quartz tubes and pressed into sputtering targets. Sr_2CrReO_6 epitaxial films were grown on $SrTiO_3$ (001) and (111) substrates by ultrahigh vacuum off-axis magnetron sputtering with a base pressure of 5×10^{-10} Torr using ultrapure Ar (99.9999%) as sputtering gas. The system is able to reliably regulate oxygen concentration down to 0.002% (20 ppm) to achieve precise control of low oxygen concentration. For the optimized sputtering pressures, this is equivalent to a precise control of O_2 partial pressure as low as 2×10^{-7} Torr. Due to the complexity of DP, a narrow window of oxygen concentration is required for the formation of the DP Sr_2CrReO_6 phase, and a delicate balance of parameters is needed for Cr/Re ordering. We optimized several correlated growth parameters including a total Ar/O_2 mixture gas pressure of 12.5 mTorr with an O_2 concentration of 0.215%, direct current (DC) sputtering with a constant current of 60 mA, a deposition rate of 0.21 Å/s, off-axis sputtering geometry, and a substrate temperature of 700 °C.

For complex materials like DP, the first important measure of film quality is stoichiometry.[20] Using Rutherford backscattering spectroscopy (RBS) at Rutgers University, we determined the composition of Sr_2CrReO_6 films to be Sr:Cr:Re = 2.07:1.00:1.00. This is very close to stoichiometric composition, and we did not observe any defects related to excess Sr from the scanning transmission electron microscopy (STEM) shown below.

In order to determine the intrinsic properties of any complex material, it is critical to ensure that the material is phase-pure and highly ordered on the atomic level. We employed two x-ray diffraction (XRD) systems for structural characterization: a Bruker D8 Advance diffractometer in Bragg-Brentano geometry and a high-resolution Bruker D8 Discover triple-axis diffractometer. Figure 1 shows XRD scans of Sr_2CrReO_6 (001) and (111) films on $SrTiO_3$ substrates. $\theta/2\theta$ scans reveal pure DP phase without any impurity peaks, such as that shown in Fig. 1(a). Using triple-axis XRD, we observe pronounced Laue oscillations near the Sr_2CrReO_6 (004) peak for the (001)-oriented film [Fig. 1(b)]. The clear Laue oscillations demonstrate a smooth film surface and sharp $Sr_2CrReO_6/SrTiO_3$ interface as well as excellent uniformity throughout the film. The out-of-plane pseudocubic lattice constant for the (001)-oriented film is $c = 7.867$ Å, which is 0.8% larger than the bulk value of $c = 7.802$ Å.[8] From an off-axis $\theta/2\theta$ scan of the same film taken for the ⟨011⟩ direction [inset of Fig. 1(b)], we obtain an in-plane lattice constant of $a = 7.807$ Å. This value matches perfectly with the $SrTiO_3$ substrate ($a = 3.904$ Å) and is in excellent agreement with bulk Sr_2CrReO_6 ($a = 5.521$ Å, $\sqrt{2}a = 7.808$ Å).[8] As a result, the Sr_2CrReO_6 (001) film exhibits a small tetragonal distortion of $c/a = 1.0077$. The exceptional crystalline quality of the Sr_2CrReO_6 films is evident in the rocking curves in Fig. 1(c). The full-width-at-half-maximum (FWHM) of the rocking curve for the Sr_2CrReO_6 (004) peak is

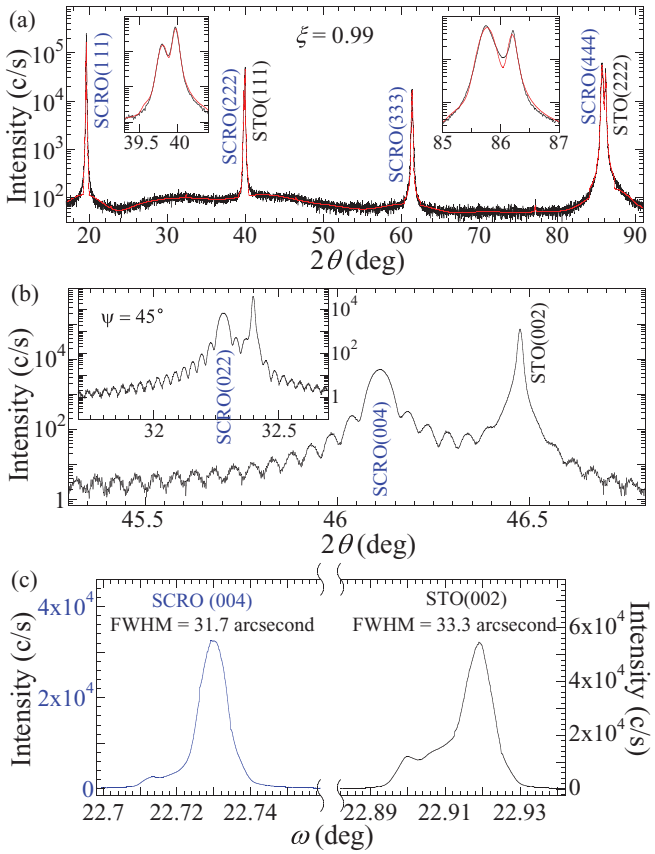

FIG. 1. (Color online) $\theta/2\theta$ XRD scans of (a) a 1220-nm thick Sr_2CrReO_6 (111) film and (b) a 190-nm thick Sr_2CrReO_6 (001) film with pronounced Laue oscillations near the Sr_2CrReO_6 (004) peak. Inset in (b) is the off-axis $\theta/2\theta$ scan of the Sr_2CrReO_6 (022) peak of the (001)-oriented film at a tilt angle $\Psi = 45°$. Cr/Re ordering parameter $\xi = 0.99 \pm 0.01$ was obtained from Rietveld refinements (red or dark grey) in (a). The insets in (a) show details of the fitting near the Sr_2CrReO_6 (222) and (444) peaks, which overlap with the substrate peaks. (c) Rocking curves of the Sr_2CrReO_6 (004) peak (blue or dark grey) and the substrate $SrTiO_3$ (002) peak (black) for a 590-nm thick Sr_2CrReO_6 (001) film.

31.7 arcseconds (0.0088°). This is the narrowest rocking curve observed to date in any DP film.[11–13,20] As a comparison, the FWHM of the rocking curve for the $SrTiO_3$ (002) peak is 33.3 arcseconds (0.0093°). The small shoulder to the left of the main peak of Sr_2CrReO_6 in Fig. 1(c) originates from a similar shoulder peak in the rocking curve of $SrTiO_3$ due to imperfections in the substrate. For all Sr_2CrReO_6 films grown under optimal conditions, the FWHM of the rocking curves is consistently similar to or slightly better than that of the $SrTiO_3$ substrate. The clear Laue oscillations and sharp rocking curves indicate that the crystalline quality of the Sr_2CrReO_6 films is comparable to that of high-quality conventional semiconductor films.[21,22]

In order to determine the Cr/Re ordering parameter ξ, we performed Rietveld refinement on the XRD scan of the (111)-oriented film [Fig. 1(a)]. Using $\xi = 2(g_{Cr/Re} - 0.5)$, where $g_{Cr/Re}$ is the refined occupancy of Cr (or Re) atoms on their correct site,[23] we obtained $\xi = 0.99 \pm 0.01$. While there are no previously reported direct measurements of ξ

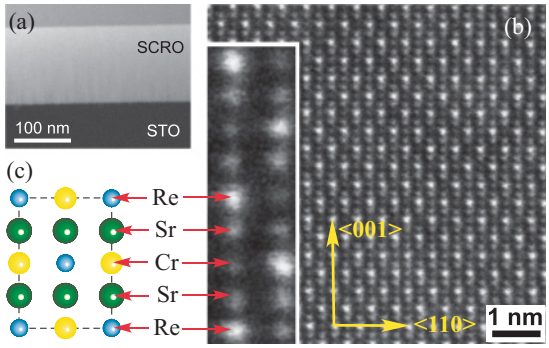

FIG. 2. (Color online) HAADF STEM images of a 134-nm-thick Sr_2CrReO_6 (001) film grown on $SrTiO_3$ viewed along the $\langle 1\bar{1}0 \rangle$ direction (a) at low magnification showing a uniform film and (b) at high magnification revealing the clear contrast of Sr, Cr, and Re atoms. The inset in (b) highlights the atomic contrast, which matches (c) the schematic projection of DP lattice along the $\langle 1\bar{1}0 \rangle$ direction.

in Sr_2CrReO_6 films, this is significantly higher than the previously reported $\xi = 0.73$ ($g_{Cr/Re} = 0.865$) for Sr_2CrReO_6 bulk samples.[17] Because the electrical and magnetic properties of DPs are highly sensitive to cation disorder, the fully ordered Sr_2CrReO_6 films allow us to probe its intrinsic properties for the first time.

Figure 2 shows aberration-corrected high-angle annular dark field (HAADF) STEM images of a Sr_2CrReO_6 (001) film taken by a FEI Titan 80-300 microscope. The low-magnification STEM image viewed along the $\langle 1\bar{1}0 \rangle$ direction in Fig. 2(a) shows a clean uniform film with little intensity variation. The interface and surface appear sharp under high magnification, corroborating the pronounced Laue oscillations in Fig. 1(b). Clear contrast in brightness is observed with three distinct shades corresponding to Sr, Cr, and Re [Fig. 2(b)]. The intensity of each atomic column is proportional to the atomic number, from which the Cr ($Z = 24$, darkest), Re ($Z = 75$, brightest), and Sr ($Z = 38$, intermediate) were identified. The inset of Fig. 2(b) is a further magnified image which matches the schematic DP lattice projection along the $\langle 1\bar{1}0 \rangle$ direction [Fig. 2(c)]. The direct observation of clear atomic arrangement validates the high crystalline quality and near perfect Cr/Re ordering in the Sr_2CrReO_6 films.

The magnetic properties of the fully ordered films were characterized via magnetic hysteresis and temperature-dependent measurements. Since film thickness is a critical factor in calculating M_S, we used combinations of Laue oscillation spacing [Fig. 1(b)], direct measurement from STEM images [Fig. 2(a)], and RBS analysis to precisely determine the film thickness, and the results from different techniques were in good agreement. Magnetic hysteresis of the Sr_2CrReO_6 films was measured by a Quantum Design Physical Property Measurement System (PPMS) with a vibrating sample magnetometer (VSM) insert and a maximum field of 14 T. From the magnetic hysteresis loop at temperature $T = 5$ K for a Sr_2CrReO_6 (001) film [Fig. 3(a)], we obtained an M_S of 1.29 μ_B/f.u., which is clearly higher than the value of 1 μ_B/f.u. expected from a ferrimagnetic alignment of Cr^{3+} $3d^3\uparrow$ and Re^{5+} $5d^2\downarrow$ ions. However, our M_S is in excellent agreement with the value of 1.28 μ_B/f.u. predicted by calculations that include spin-orbit coupling.[19] This result directly confirms

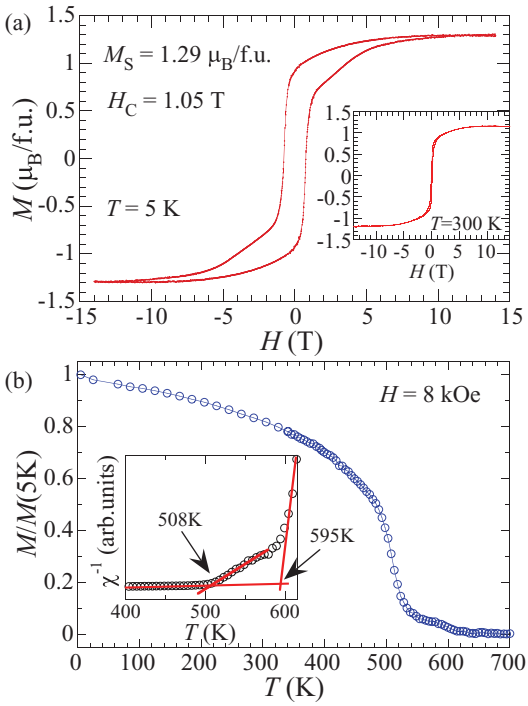

FIG. 3. (Color online) (a) In-plane hysteresis loop at $T = 5$ K and (b) M vs T curve at $H = 0.8$ T of a 1220-nm-thick Sr_2CrReO_6 (001) film. The measured M_S and coercivity (H_C) are 1.29 μ_B/f.u. and 1.05 T at 5 K, respectively. The inset in (a) is the M vs H curve at $T = 300$ K with a $M_S = 1.14$ μ_B/f.u and $H_C = 890$ Oe. The inset in (b) is the T-dependence of inverse magnetic susceptibility (χ^{-1}), which gives a T_C of 508 K for the majority phase and a secondary T_C of 595 K.

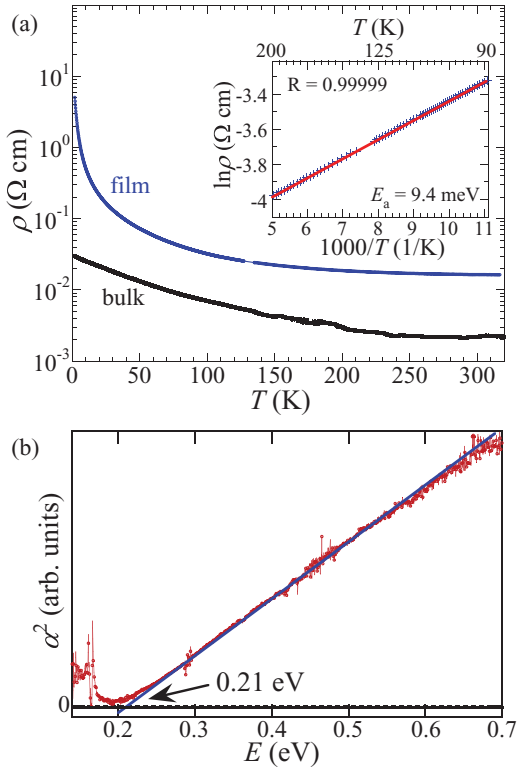

FIG. 4. (Color online) (a) Semi-log plots of ρ vs T of bulk Sr_2CrReO_6 (black) and a 200-nm-thick Sr_2CrReO_6 (001) film (blue or dark grey) measured by standard four-probe measurements. The inset is an $\ln\rho$ vs $1000/T$ plot, which has an almost perfect linear fit with a linear correlation coefficient $R = 0.99999$. The activation energy was determined to be $E_a = 9.4$ meV. (b) Tauc plot α^2 vs E of a FTIR absorption spectrum of a 200-nm-thick Sr_2CrReO_6 (001) film, which gives a clear gap of $E_g = 0.21$ eV.

the presence of strong spin-orbit coupling in Sr_2CrReO_6. The coercivity (H_C) at 5 K is 1.05 T, indicating that Sr_2CrReO_6 is a hard ferrimagnet at low temperatures. However, H_C decreases significantly to 890 Oe at 300 K, suitable for room temperature magneto-electronic applications.

Figure 3(b) shows an M vs T curve of a Sr_2CrReO_6 film measured by a LakeShore variable-temperature VSM at an applied field of 8 kOe. From the inverse magnetic susceptibility (χ^{-1}) between 400 and 620 K [inset of Fig. 3(b)], we determined a primary transition at 508 K. In addition, there is a small secondary transition at 595 K. As a comparison, the previously reported T_C is 620−635 K for bulk Sr_2CrReO_6[15,16] and 481 K for Sr_2CrReO_6 films.[13] The secondary phase with higher T_C could come from regions in the vicinity of a small number of antiphase boundaries where stronger exchange interaction may exist and enhance T_C.

Figure 4(a) shows the semi-log plots of electrical resistivity (ρ) vs T for a bulk Sr_2CrReO_6 sample and a Sr_2CrReO_6 (001) film. The bulk resistivity at room temperature is 2.1 mΩ cm. It exhibits a shallow minimum at 280 K and increases at lower temperatures, in qualitative agreement with Kato *et al.*[15] For the Sr_2CrReO_6 film, the resistivity increases by more than two orders of magnitude from $\rho = 16.2$ mΩ cm at 300 K to $\rho = 5.05$ Ω cm at 2 K. This behavior is characteristic of a semiconductor (or insulator) with a gap at the Fermi level. The inset in Fig. 4(a) shows an $\ln\rho$ vs $1000/T$ plot over a range of 90 to 200 K, which gives an almost perfect linear fit. This kind of T-dependence is commonly seen in semiconductors due to thermally activated transport,[24] which follows the relationship $\rho \propto \exp(E_a/k_BT)$, where E_a is the activation energy. For doped semiconductors, E_a is the energy difference between donor (acceptor) levels and the conduction (valence) band edge. From the linear fit we determined an activation energy $E_a = 9.4$ meV. Although the nature of the dopant states cannot be determined from transport measurements, the small value of E_a is comparable to those of dopant levels in conventional semiconductors like GaAs. For $T < 90$ K, the $\ln\rho$ vs $1000/T$ plot is no longer linear, but very good linear fits can be obtained for $\ln\rho$ vs $(1000/T)^{0.25}$ from 55 to 90 K and for $\ln\rho$ vs $(1000/T)^{0.20}$ from 6 to 25 K. This indicates a variable-range hopping transport, as observed in many doped semiconductors at low temperatures.[25]

To further corroborate the conclusion that Sr_2CrReO_6 is a semiconductor rather than a metal, Fourier-transform infrared (FTIR) transmission spectroscopy was performed on a 200-nm thick Sr_2CrReO_6 (001) film grown on a double-side polished $SrTiO_3$ substrate. Figure 4(b) shows the α^2 vs E plot where α is the absorption coefficient and E is the photon energy.[26] This plot clearly demonstrates a direct band gap of $E_g = 0.21$ eV in the Sr_2CrReO_6 film. The features below 0.17 eV are likely due to phonon modes. The noise in the vicinities of 0.29 eV

and 0.44−0.50 eV can be attributed to water vapor and CO_2 present in the FTIR chamber.

An obvious question is why until now has Sr_2CrReO_6 been classified as a metal instead of a semiconductor. We believe that in previous studies the significant levels of disorder resulted in ambiguous transport properties, not so different from those seen in conventional semiconductors with high doping levels such as $Ga_{1-x}Mn_xAs$.[27] In fact, nearly all previously published ρ vs T curves exhibit a minimum between 130 and 300 K.[10,11,13,15] However, since the changes in ρ are only weakly T-dependent ($\rho_{5K}/\rho_{300K} < 3$), Sr_2CrReO_6 was considered a (bad) metal with defects, which caused the resistivity to go up at low temperatures. The fact that our highly ordered Sr_2CrReO_6 films exhibit $\rho_{2K}/\rho_{300K} > 100$ reveals the true semiconducting nature of Sr_2CrReO_6.

The mechanism responsible for the semiconducting behavior in Sr_2CrReO_6 is less clear since electronic interaction in strongly correlated systems is very complicated.[28] Given the presumed Re^{5+} valence state the minority spin Re ($5d$) t_{2g} band should be two-thirds filled, and thus metallic conductivity is expected. Disorder in these films appears to be relatively low, so Anderson localization is not a likely explanation for the semiconducting behavior nor is there evidence for orbital ordering in bulk samples of Sr_2CrReO_6.[16] However, the subtle tetragonal distortion of these films should be further investigated to see if it plays a role. A plausible explanation is that Sr_2CrReO_6 is a Mott semiconductor (insulator), but further investigations of high-quality Sr_2CrReO_6 films coupled with theoretical modeling are needed to better understand this intriguing behavior.

This Rapid Communication is supported by the Center for Emergent Materials at the Ohio State University, a NSF Materials Research Science and Engineering Center (DMR-0820414). We thank M. Randeria, A. Mukherjee, O. Erten, and O. N. Meetei for fruitful discussions.

*fyyang@mps.ohio-state.edu

[1] H. Dery, P. Dalal, L. Cywiński, and L. J. Sham, Nature **447**, 573 (2007).
[2] S. A. Wolf, D. D. Awschalom, R. A. Buhrman, J. M. Daughton, S. von Molnár, M. L. Roukes, A. Y. Chtchelkanova, and D. M. Treger, Science **294**, 1488 (2001).
[3] K. Ando, Science **312**, 1883 (2006).
[4] A. H. MacDonald, P. Schiffer, and N. Samarth, Nat. Mater. **4**, 195 (2005).
[5] R. A. de Groot, F. M. Mueller, P. G. van Engen, and K. H. J. Buschow, Phys. Rev. Lett. **50**, 2024 (1983).
[6] Y. Yamada, K. Ueno, T. Fukumura, H. T. Yuan, H. Shimotani, Y. Iwasa, L. Gu, S. Tsukimoto, Y. Ikuhara, and M. Kawasaki, Science **332**, 1065 (2011).
[7] K. L. Kobayashi, T. Kimura, H. Sawada, K. Terakura, and Y. Tokura, Nature **395**, 677 (1998).
[8] D. Serrate, J. M. De Teresa, and M. R. Ibarra, J. Phys.: Condens. Matter **19**, 023201 (2007).
[9] G. Blamire, J. L. MacManus-Driscoll, N. D. Mathur, and Z. H. Barber, Adv. Mater. **21**, 3827 (2009).
[10] H. Asano, N. Kozuka, A. Tsuzuki, and M. Matsui, Appl. Phys. Lett. **85**, 263 (2004).
[11] S. Chakraverty, A. Ohtomo, and M. Kawasaki, Appl. Phys. Lett. **97**, 243107 (2010).
[12] S. Geprägs, F. D. Czeschka, M. Opel, S. T. B. Goennenwein, W. Yu, W. Mader, and R. Gross, J. Magn. Magn. Mater. **321**, 2001 (2009).
[13] J. Orna, L. Morellon, P. A. Algarabel, J. A. Pardo, C. Magen, M. Varela, S. J. Pennycook, J. M. De Teresa, and M. R. Ibarra, J. Magn. Magn. Mater. **322**, 1217 (2010).
[14] M. Opel, S. Geprägs, E. P. Menzel, A. Nielsen, D. Reisinger, K.-W. Nielsen, A. Brandlmaier, F. D. Czeschka, M. Althammer, M. Weiler, S. T. B. Goennenwein, J. Simon, M. Svete, W. T. Yu, S.-M. Hühne, W. Mader, and R. Gross, Phys. Status Solidi A **208**, 232 (2011).
[15] H. Kato, T. Okuda, Y. Okimoto, Y. Tomioka, Y. Takenoya, A. Ohkubo, M. Kawasaki, and Y. Tokura, Appl. Phys. Lett. **81**, 328 (2002).
[16] J. M. De Teresa, D. Serrate, C. Ritter, J. Blasco, M. R. Ibarra, L. Morellon, and W. Tokarz, Phys. Rev. B **71**, 092408 (2005).
[17] J. M. De Teresa, J. M. Michalik, J. Blasco, P. A. Algarabel, M. R. Ibarra, C. Kapusta, and U. Zeitler, Appl. Phys. Lett. **90**, 252514 (2007).
[18] T. K. Mandal, C. Felser, M. Greenblatt, and J. Kübler, Phys. Rev. B **78**,134431 (2008).
[19] G. Vaitheeswaran, V. Kanchana, and A. Delin, Appl. Phys. Lett. **86**, 032513 (2005).
[20] A. J. Hauser, R. E. A. Williams, R. A. Ricciardo, A. Genc, M. Dixit, J. M. Lucy, P. M. Woodward, H. L. Fraser, and F. Y. Yang, Phys. Rev. B **83**, 014407 (2011).
[21] L. Liu and J. H. Edgar, Mater. Sci. Eng., R **37**, 61 (2002).
[22] T. L. Tran, F. Hatami, W. T. Masselink, V. P. Kunets, and G. J. Salamo, J. Electron. Mater. **37**, 1799 (2008).
[23] Y. H. Huang, M. Karppinen, H. Yamauchi, and J. B. Goodenough, Phys. Rev. B **73**, 104408 (2006).
[24] J. F. Shackelford, *Introduction to Materials Science for Engineers*, 7th ed. (Prentice Hall, New York, 2008), Ch. 17.
[25] C. Michel, S. D. Baranovskii, P. J. Klar, P. Thomas, and B. Goldlücke, Appl. Phys. Lett. **89**, 112116 (2006).
[26] A. J. Hauser, J. Zhang, L. Mier, R. A. Ricciardo, P. M. Woodward, T. L. Gustafson, L. J. Brillson, and F. Y. Yang, Appl. Phys. Lett. **92**, 222901 (2008).
[27] A. Van Eschyz, J. De Boeck, L. Van Bockstal, R. Bogaerts, F. Herlach, and G. Borghs, J. Phys.: Condens. Matter **9**, L361 (1997).
[28] J. Winterlik, G. H. Fecher, C. A. Jenkins, C. Felser, C. Mühle, K. Doll, M. Jansen, L. M. Sandratskii, and J. Kübler, Phys. Rev. Lett. **102**, 016401 (2009).